FULL PAPER

Dalton
www.rsc.org/dalton

Synthesis and structural characterization of luminescent gold(I) derivatives with an unsymmetric diphosphine

Manuel Bardají,†[a] Peter G. Jones,[b] Antonio Laguna,*[a] M. Dolores Villacampa[a] and Noelia Villaverde[a]

[a] *Departamento de Química Inorgánica, Instituto de Ciencia de Materiales de Aragón, Universidad de Zaragoza-CSIC, E-50009 Zaragoza, Spain. E-mail: alaguna@posta.unizar.es; Fax: + 34 976 761187; Tel: + 34 976 761185*

[b] *Institut für Anorganische und Analytische Chemie der Technischen Universität, Postfach 3329, D-38023 Braunschweig, Germany*

Received 31st July 2003, Accepted 17th September 2003
First published as an Advance Article on the web 26th September 2003

We have synthesised a series of mono-bridged digold(I) derivatives with an unsymmetric diphosphine, namely, $[(\mathrm{AuX})_2(\mu\text{-}\mathrm{P^iPr_2CH_2PPh_2})]$ (X = Cl, Br, I, C_6F_5, $S_2CN(CH_2Ph)_2$) and the mononuclear gold(III) complex $[\mathrm{Au}(C_6F_5)_3(\mathrm{P^iPr_2CH_2PPh_2})]$. X-ray diffraction studies show intramolecular gold(I)–gold(I) interactions of 3.4179(2), 3.1660(2) and 3.0926(3) Å, respectively, for X = Cl, Br and C_6F_5. The pentafluorophenyl derivative emits at 445 nm at room temperature in the solid state; this compound and the halo-derivatives are emissive at low temperature in the range 440–486 nm. We have also prepared doubly-bridged diauracycles, namely, $[\mathrm{Au_2X_2}(\mu\text{-}\mathrm{P^iPr_2CH_2PPh_2})_2]$ (X = Cl, Br, I) and $[\mathrm{Au_2}(\mu\text{-}\mathrm{P^iPr_2CH_2PPh_2})_2]\mathrm{A_2}$ (A = CF_3SO_3, ClO_4). The crystal structure of the iodo derivative displays three-coordinated gold centres in a T-shaped geometry, with a gold–gold distance of 2.9931(6) Å and a gold–iodo distance of 3.0999(6) Å, whilst the triflate derivative displays di-coordinated gold centres and a gold–gold distance of 2.9838(5) Å. All the derivatives are intensely photoluminescent in the visible range, with the emission maxima between 480 and 513 nm at 298 K and 459–508 nm at 77 K. The emission energies and the gold–gold distances are not directly related.

Introduction

Intramolecular gold(I)–gold(I) interactions in the range 2.9–3.6 Å have been reported in mono- or doubly-bridged dinuclear complexes. Values from 20 to 50 kJ mol^{-1}, close to those found for hydrogen bonds, have been obtained for these gold(I)–gold(I) interactions by analysis of temperature-dependent NMR measurements. Theoretical studies have suggested correlation effects enhanced by relativistic effects to explain these aurophilic interactions.[1] It has been predicted that the strength of these contacts should increase with the softness of the ligand, and this has been confirmed experimentally in some series of derivatives.[2]

Since the first report on the photoluminescence of $[\mathrm{Au_2}(\mu\text{-dppm})_2]^{2+}$ (dppm = bis(diphenylphosphino)methane),[3] polynuclear phosphino gold(I) complexes have received much attention because they display long-lived emissions in the visible region, which have been usually attributed to excited states involving gold–gold bonding.[4] However, the intermetallic separation does not appear to play a significant role in determining the energy of the emission, whilst the auxiliary ligands, the counter-ion or the solvent can dramatically affect the optical properties. In fact, recent studies on $[\mathrm{Au_2}(\mu\text{-dcpm})_2]^{2+}$ (dcpm = bis(dicyclohexylphosphino)methane) point to exciplexes to explain the photoluminescence.[5]

In this work we report the first mono- and doubly-bridged dinuclear gold(I) derivatives with an unsymmetric diphosphine, namely, $[(\mathrm{AuX})_2(\mu\text{-}\mathrm{P^iPr_2CH_2PPh_2})]$, $[\mathrm{Au_2X_2}(\mu\text{-}\mathrm{P^iPr_2CH_2PPh_2})_2]$ and $[\mathrm{Au_2}(\mu\text{-}\mathrm{P^iPr_2CH_2PPh_2})_2]\mathrm{A_2}$, and also a mononuclear gold(III) derivative. The pentafluorophenyl gold(I) complex and all the doubly-bridged diphosphine complexes are intensely photoluminescent at room and low temperature in the visible range, whilst most of the other mono-bridged gold(I) derivatives are only emissive at low temperature. We have carried out X-ray diffraction studies of five derivatives, three mono-bridged which display gold–gold distances of 3.4179(2), 3.1660(2) and 3.0926(3) Å, respectively, for Cl, Br and C_6F_5, and two doubly-bridged with gold–gold distances of 2.9931(6) and 2.9838(5) Å, respectively for I and CF_3SO_3.

Results and discussion

Synthesis and characterization of monobridged derivatives

The reaction of diisopropylphosphine(diphenylphosphine)-methane with the appropriate gold(I) complex containing an easily displaceable ligand, in molar ratio 1 : 2 in dichloromethane, leads to the monobridged dinuclear gold(I) complexes **1**–**4** (see Scheme 1). Complex **1** reacts with dithiocarbamate salts to give the corresponding dithiocarbamato derivative **5** by substitution of the chloro ligands. The reaction of the unsymmetrical ditertiary phosphine with $[\mathrm{Au}(C_6F_5)_3(\mathrm{tht})]$ affords the mononuclear gold(III) complex **6**. These derivatives are air- and moisture-stable white (**1**–**4**, **6**) or yellow (**5**) solids at room temperature.

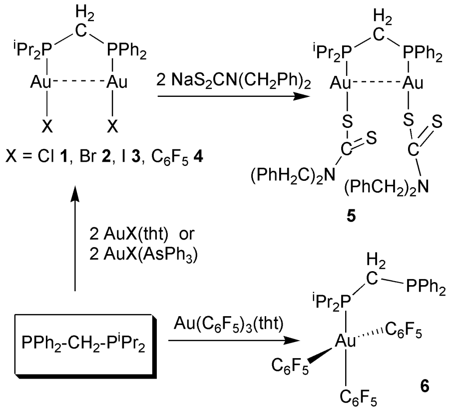

Scheme 1

---

† Present and permanent address: Departamento de Química Inorgánica, Facultad de Ciencias, Universidad de Valladolid, 47005-Valladolid, Spain.

DOI: 10.1039/b309116c

Table 1 $^{31}P\{^1H\}$ NMR data for monobridged complexes **1**–**6**

Complex	$\delta(PPh_2)$	$\delta(P^iPr_2)$
$PPh_2\,CH_2P^iPr_2$	−19.2	−3.9
$[(AuCl)_2(\mu\text{-}P^iPr_2CH_2PPh_2)]$	39.2	54.4
$[(AuBr)_2(\mu\text{-}P^iPr_2CH_2PPh_2)]$	35.4	51.4
$[(AuI)_2(\mu\text{-}P^iPr_2CH_2PPh_2)]$	32.6	51.6
$[\{Au(C_6F_5)\}_2(\mu\text{-}P^iPr_2CH_2PPh_2)]$	37.5	54.8
$[\{Au(S_2CNR_2)\}_2(\mu\text{-}P^iPr_2CH_2PPh_2)]$	31.1	54.4
$[Au(C_6F_5)_3(P^iPr_2CH_2PPh_2)]$	−27.5	38.4

They were readily characterised by elemental analysis, mass, IR and NMR spectroscopies (see Experimental section). Their IR spectra show absorptions at 326 (**1**) cm^{-1} due to ν(Au–Cl),[6] or at 955 and 792 (**4**) or 966 and 792 (**6**) cm^{-1} from the pentafluorophenyl groups.[7] Their acetone solutions are non-conducting. The ^{1}H NMR spectra show two doublets of doublets *ca.* 1.16 and 1.26 ppm for two sets of inequivalent methyl groups, which are simplified to two doublets in a phosphorus decoupled experiment; in this experiment a septuplet or a multiplet is found for the CH of the isopropyl group and a singlet for the methylene bridge. Two slightly different pentafluorophenyl groups are seen for complex **4** and a unique $Au(C_6F_5)_3$ unit for complex **6**.

In the phosphorus NMR spectra an AX spin system is observed, strongly low-field shifted when the diphosphine is coordinated (see Table 1). Chemical shifts sequences are different, $Au(C_6F_5)_3$ < AuBr, AuI < AuCl, AuC_6F_5, AuS_2CNR_2, for bis(isopropyl)phosphino group whilst AuS_2CNR_2 < AuI < AuBr < AuC_6F_5 < AuCl is found for diphenylphosphino group, which is therefore more sensitive to the gold coordinated fragment. The phosphorus NMR spectrum of **6** confirms that the gold(III) unit is coordinated to the bis(isopropyl)phosphine arm; curiously the addition of more gold(III) precursor does not lead to the expected dinuclear derivative, as found for dppm (bis(diphenylphosphino)methane), but complex **6** is recovered from solution. The mass spectra always show the peak corresponding to the $[M - X]^+$ fragment (X = Cl, Br, I, C_6F_5, S_2CNR_2 and C_6F_5, respectively, for complexes **1**–**6**).

X-Ray crystal structure determination of 1, 2 and 4

The molecular structures of these complexes are similar and those of complexes **1** and **4** are shown in Figs. 1 and 2, respectively. Selected bonds and angles for complexes **1**, **2** and **4** are summarised in Table 2. Complexes **1** and **2** are not isostructural; they crystallise with different amounts of solvent. The molecular structures consist of discrete dinuclear molecules with an almost linear coordination for the gold(I) centres, which is typical of dinuclear dppm gold(I) derivatives.[8] The molecules display short gold–gold distances, following the sequence: C_6F_5 < Br < Cl. It is clear in this case that steric hindrance is not controlling aurophilic interactions (bigger ligands produce shorter gold–gold distances). Electronic effects have been reported to increase aurophilic attractions with the softness of the ligands, as reported for the series $(AuX)_2(\mu\text{-dpph})$ (X = Cl, I; dpph = bis(diphenylphosphino)hexane),[2b] AuX(TPA) (X = Cl, Br; TPA = *P*-(1,3,5-triaza-7-phosphaadamantane)),[2c] AuX(CNxylyl-*o*) (X = Cl, Br, I, CN),[2d] $[\{AuX(PPhMe_2)\}_2]$ (X = Cl, Br, I),[2e] and $AuX(PPh_2CCH)$ (X = Cl, I).[2f] The pentafluorophenyl ligand is quite big and highly electronegative but the shortest gold–gold distance is displayed. It can be seen in Fig. 2 that pentafluorophenyl rings are almost parallel (angle of 12°) and with a distance of about 3.5 Å and therefore an additional stabilization could occur by π–π interactions. A similar result was found in $[\{Au(C_6F_5)\}_2(\mu\text{-dppm})]$, which displays a gold–gold distance as short as 3.163(1) Å.[8e]

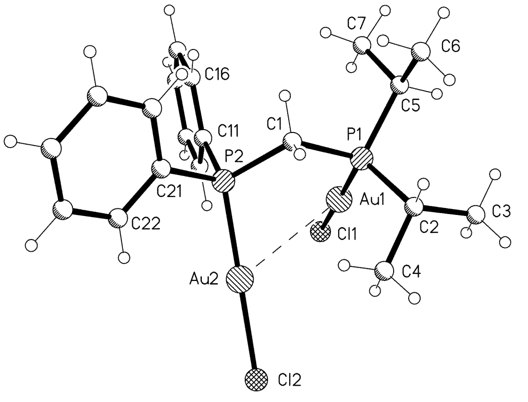

Fig. 1 Molecular structure of the dinuclear monobridged derivative **1**.

Table 2 Selected bond distances (Å) and angles (°) within molecules $[(AuX)_2(\mu\text{-PPh}_2CH_2P^iPr_2)]$, X = Cl **1**, Br **2**, C_6F_5 **4**

Complex 1			
Au(1)–P(1)	2.2358(7)	P(1)–Au(1)–Cl(1)	176.31(2)
Au(1)–Cl(1)	2.3008(7)	P(2)–Au(2)–Cl(2)	175.67(2)
Au(2)–P(2)	2.2375(6)	P(1)–Au(1)–Au(2)	80.818(17)
Au(2)–Cl(2)	2.2985(6)	Cl(1)–Au(1)–Au(2)	102.441(17)
Au(1)–Au(2)	3.4179(2)	P(2)–Au(2)–Au(1)	73.666(16)
		Cl(2)–Au(2)–Au(1)	109.136(17)
Complex 2			
Au(1)–P(1)	2.2445(7)	P(1)–Au(1)–Br(1)	175.94(2)
Au(1)–Br(1)	2.4198(3)	P(2)–Au(2)–Br(2)	174.08(2)
Au(1)–Au(2)	3.1660(2)	P(1)–Au(1)–Au(2)	86.853(19)
Au(2)–P(2)	2.2403(7)	Br(1)–Au(1)–Au(2)	93.520(10)
Au(2)–Br(2)	2.4069(3)	P(2)–Au(2)–Au(1)	76.759(18)
		Br(2)–Au(2)–Au(1)	109.098(10)
Complex 4			
Au(1)–C(1)	2.044(5)	C(1)–Au(1)–P(1)	175.59(14)
Au(1)–P(1)	2.2682(15)	C(11)–Au(2)–P(2)	175.70(16)
Au(1)–Au(2)	3.0926(3)	C(1)–Au(1)–Au(2)	92.98(14)
Au(2)–C(11)	2.046(6)	P(1)–Au(1)–Au(2)	91.23(4)
Au(2)–P(2)	2.2787(15)	C(11)–Au(2)–Au(1)	95.54(14)
		P(2)–Au(2)–Au(1)	84.03(4)

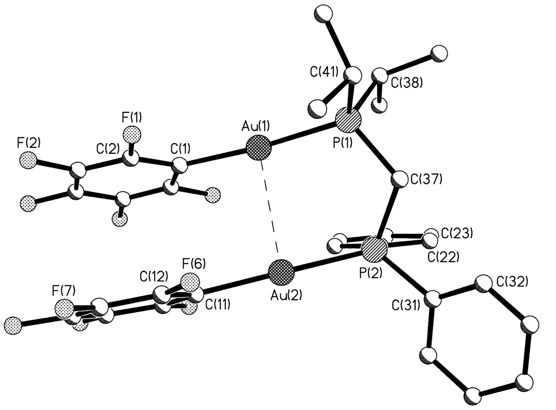

Fig. 2 Molecular structure of the dinuclear monobridged derivative **4**; H-atoms are omitted for clarity.

The Au–P distances display a *trans* influence in the sequence Cl < Br < C_6F_5, for both phosphine arms. The isopropylphosphino fragment induces a stronger *trans* influence compared to the phenylphosphino fragment over the Au–X distance for X = Cl, Br, whilst there is no difference for the pentafluorophenyl derivative. Complexes **1**, **2** and **4** display several C–H ··· X contacts, X = Cl, Br, F or O (solvent), that could be interpreted as hydrogen bonds. In particular, there are extremely short contacts involving the hydrogens of the CH_2 group; normalised values are H1A ··· Cl1 2.45 Å for **1** and H1A ··· O91(acetone) 2.39 Å for **2**. In addition, there is a weak intermolecular interaction C–H ··· Au, (H ··· Au 2.93 Å and

Table 3 Hydrogen bonds for complexes **1**, **2** and **4** (Å and °)

Compound **1**

D–H ··· A	*d*(D–H)	*d*(H ··· A)	*d*(D ··· A)	∠(DHA)
C(1)–H(1A) ··· Cl(1)#1	0.99	2.54	3.518(3)	170.1
C(1)–H(1B) ··· Cl(2)#1	0.99	2.84	3.790(2)	161.3
C(6)–H(6C) ··· Cl(2)#1	0.98	2.92	3.789(3)	147.9
C(26)–H(26) ··· Cl(2)#1	0.95	2.83	3.771(3)	170.5
C(5)–H(5) ··· Cl(1)#2	1.00	2.92	3.611(3)	127.0
C(6)–H(6A) ··· Cl(1)#2	0.98	2.98	3.605(3)	122.3
C(99)–H(99B) ··· Cl(1)#3	0.98	2.97	3.835(4)	147.2

Symmetry transformations used to generate equivalent atoms: #1 x, $-y + 1/2$, $z + 1/2$; #2 $-x + 2$, $-y + 1$, $-z + 1$. #3 $-x + 1$, $-y + 1$, $-z + 1$.

Compound **2**

D–H ··· A	*d*(D–H)	*d*(H ··· A)	*d*(D ··· A)	∠(DHA)
C(1)–H(1A) ··· O(91)	0.99	2.45	3.253(4)	137.4
C(2)–H(2) ··· O(91)	1.00	2.55	3.401(4)	142.4
C(24)–H(24) ··· Br(1)#1	0.95	2.96	3.797(3)	148.2
C(23)–H(23) ··· Br(1)#2	0.95	3.01	3.952(3)	170.5
C(1)–H(1B) ··· Br(2)#2	0.99	2.93	3.870(3)	158.4
C(6)–H(6C) ··· Br(2)#2	0.98	3.14	4.027(3)	150.8
C(16)–H(16) ··· Br(2)#2	0.95	3.14	4.016(3)	153.3
C(22)–H(22) ··· Br(2)#2	0.95	2.96	3.799(3)	148.3
C(93)–H(93C) ··· Br(2)#2	0.98	3.06	3.789(5)	132.1

Symmetry transformations used to generate equivalent atoms: #1 $x - 1/2$, $y - 1/2$, z; #2 $-x + 3/2$, $y - 1/2$, $-z + 1/2$.

Compound **4**

D–H ··· A	d(D–H)	d(H ··· A)	d(D ··· A)	∠(DHA)
C(37)–H(37B) ··· F(4)#1	0.97	2.48	3.436(6)	169.9
C(35)–H(35) ··· F(4)#2	0.93	2.48	3.160(7)	130.5
C(32)–H(32) ··· F(4)#1	0.93	2.61	3.275(6)	128.7
C(43)–H(43C) ··· Au(2)#3	0.96	2.93	3.852(6)	162.6

Symmetry transformations used to generate equivalent atoms: #1 $-x$, $y + 1/2$, $-z + 1/2$; #2 $-x$, $-y$, $-z + 1$; #3 x, $-y + 1/2$, $z - 1/2$.

C–H ··· Au 163°), involving one hydrogen of a CH_3 group in compound **4** (see Table 3).

Synthesis and characterization of doubly-bridged derivatives

The reaction of the unsymmetrical diphosphine with the gold(I) complex [AuXL] or $[Au(tht)_2]A$ in molar ratio 1 : 1 in dichloromethane, leads to the doubly-bridged dinuclear gold(I) complexes **7**–**11** (see Scheme 2). These derivatives are air-and moisture-stable white (**7**–**8**, **10**–**11**) or yellow (**9**) solids at room temperature. They were characterised by elemental analysis, conductivity, mass, IR and NMR spectroscopies (see Experimental section). The main features are: (a) the IR spectrum of **7** shows an absorption at 326 cm^{-1} arising from coordination of chloride; besides, the spectra of derivatives **10** and **11** show absorptions, respectively, at 1253 and 637 cm^{-1}, 1092 (s) and 623 cm^{-1}, corresponding to ionic triflate and perchlorate; (b) their acetone solutions behave as 1 : 2 electrolytes for complexes **10**–**11**, and are essentially non-conducting for **7**–**9** (although some molar conductivity is observed). Therefore halides are coordinated to the gold(I) centres but triflate or perchlorate are not. This is important because the vast majority of gold(I) complexes are two-coordinate, whilst three- and four-coordinate species are uncommon.[9]

Moreover, NMR spectra confirmed the presence of head–head and head–tail isomers (see Fig. 3) in *ca.* the following proportion (% head–head isomer : % head–tail isomer): 70 : 30 (**7**), 60 : 40 (**8**), 75 : 25 (**9**), 50 : 50 (**10**), 65 : 35 (**11**). Phosphorus NMR spectra showed AA′XX′ spin systems with two sets of very close resonances, summarised in Table 4. The first half system (AA′ and XX′ parts are equal in AA′XX′ spin systems) consists of four lines (close to a doublet of doublets) with a $^2J(PPh_2–P^iPr_2)$ around 300 Hz because of *trans* coupling and a $^2J(PPh_2–P^iPr_2)$ around 45 Hz due to coupling in the same diphosphine, assigned to the head–tail isomer ($^4J(PPh_2–PPh_2) = {}^4J(P^iPr_2–P^iPr_2) \approx 0$). The second half system consists of a pseudo-triplet (with inverted intensity 2 : 1 : 2) or a triplet (less intense) in the middle of a doublet, due to strong $^2J(PPh_2–PPh_2)$ and $^2J(P^iPr_2–P^iPr_2)$ (found by calculation in the range 255–295 Hz), and $^2J(PPh_2–P^iPr_2)$ *ca.* 50 Hz in the same diphosphine, from the head–head isomer (see Experimental section).[10] Now, the chemical shifts sequence is the same for both phosphine arms: I < Br < Cl < ClO_4, CF_3SO_3. The ^1H and $^1H\{^{31}P\}$ NMR

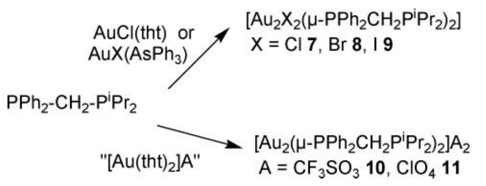

Scheme 2

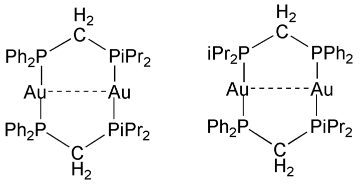

Fig. 3 Head–head and head–tail isomers.

Table 4 $^{31}P\{^1H\}$ NMR data for doubly-bridged complexes **7**–**11**.[a]

Complex	$\delta(PPh_2)$	$\delta(P^iPr_2)$
7a	33.2	59
7b	33.7	59.1
8a	31.3	57.6
8b	31.7	57.7
9a	27.6	53.1
9b	28.9	53.6
10a	37.6	61.2
10b	37.5	62.2
11a	36.5	59.6
11b	36.7	60.8

[a] Head–head isomer is denoted **a**; head–tail isomer is denoted **b**.

spectra are similar to those found in monobridged derivatives **1**–**6** but more complicated because of the presence of two isomers (two CH_2 resonances can be distinguished for derivatives **9**–**11**).

X-Ray crystal structure determination of 9 and 10

The molecular structures of complexes **9** and **10** are shown in Figs. 4 and 5, respectively. Selected bonds and angles are summarised in Table 5. The molecules are eight-membered diauracycles in a chair conformation; both display crystallographic inversion symmetry. Therefore we have found the head–tail isomer for both complexes, although in solution a mixture was always found; the redissolution of the crystals again led to a mixture of isomers in solution. This fact can be explained because of phosphine exchange in solution (fluxionality in phosphino gold(I) derivatives is not uncommon), although a mixture of isomers in the crystals can not be excluded. They display short gold–gold intramolecular interactions of 2.9931(6) and 2.9838(5) Å respectively for **9** and **10**, which are shorter than those found in the monobridged complexes; there are no intermolecular gold–gold interactions.

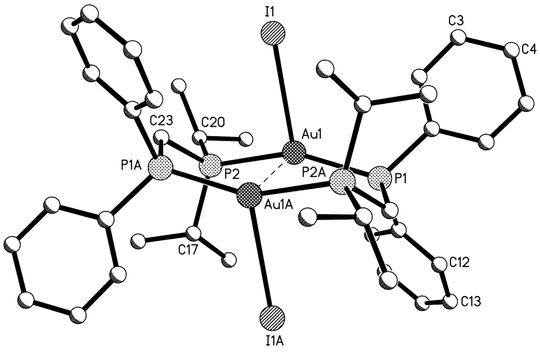

Fig. 4 Molecular structure of the dinuclear doubly-bridged derivative **9**; H-atoms are omitted for clarity.

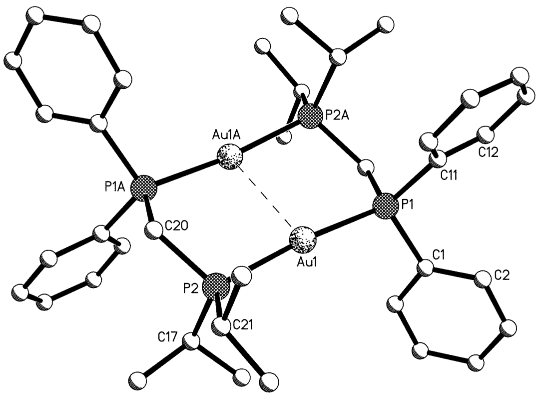

Fig. 5 Structure of the dinuclear doubly-bridged cation of **10**; H-atoms are omitted for clarity.

Table 5 Selected bond distances (Å) and angles (°) within molecules $[Au_2I_2(\mu\text{-}P^iPr_2CH_2PPh_2)_2]$ **9** and $[Au_2(\mu\text{-}P^iPr_2CH_2PPh_2)_2](CF_3SO_3)_2$ **10**

Complex **9**

Au(1)–P(1)	2.3086(19)	P(1)–Au(1)–I(1)	113.05(5)
Au(1)–P(2)	2.3302(19)	P(2)–Au(1)–I(1)	92.48(5)
Au(1)–Au(1)#1	2.9931(6)	Au(1)#1–Au(1)–I(1)	95.563(18)
Au(1)–I(1)	3.0999(6)	P(1)–Au(1)–Au(1)#1	92.95(5)
P(1)–Au(1)–P(2)	154.47(7)	P(2)–Au(1)–Au(1)#1	84.21(5)

Symmetry transformations used to generate equivalent atoms: #1 $-x + 1, -y, -z + 2$.

Complex **10**

Au(1)–P(1)	2.2993(14)	P(1)–Au(1)–P(2)	172.32(5)
Au(1)–P(2)	2.3020(14)	P(1)–Au(1)–Au(1)#1	92.13(4)
Au(1)–Au(1)#1	2.9838(5)	P(2)–Au(1)–Au(1)#1	89.70(4)

Symmetry transformations used to generate equivalent atoms: #1 $-x + 2, -y + 1, -z + 1$.

Additionally, gold centres in complex **9** are three-coordinated in a T-shaped AuP_2I geometry with a Au–I bond length of 3.0999(6) Å, longer than a typical Au–I bond length. This geometry is typical of $[Au_2X_2(\mu\text{-diphosphine})_2]$ (X = halide),[9] although different configurations have been reported for iodo derivatives: (a) T-shaped as adopted for derivative **9** in $[Au_2I_2(\mu\text{-dcpm})_2]$ (Au–I: 2.9960(7) Å);[5b] (b) T-shaped geometry with the two gold centres symmetrically or asymmetrically bridged by one iodo, as reported in $[Au_2I(\mu\text{-dppm})_2]I$ (Au–I: 3.127(2) and 3.196(2) Å)[11] and in $[Au_2I(\mu\text{-dppm})_2][Au(CN)_2]$ (Au–I: 3.161(3) and 3.342(3) Å);[12] (c) T-shaped as shown in derivative **9**, but additionally one iodo bridges two dinuclear units (one gold is tetra-coordinated) as found in $[Au_2I_2(\mu\text{-dmpe})_2]$ (dmpe = 1,2-bis(dimethylphosphino)ethane; Au–I: 3.151(1)–3.425(1) Å).[13] The P–Au–P angle in **9**, 154.47(7)°, deviates from linear geometry; this value is in line with those found in related three-coordinated gold(I) compounds such as 155.9(1)° in $[Au_2Cl_2(\mu\text{-dppm})_2]$,[14] 156.5(1)° in $[Au_2Br_2(\mu\text{-dppm})_2]$,[11] or 157.93(7)° in $[Au_2I_2(\mu\text{-dcpm})_2]$.[5b] The closest Au ··· anion contact in **10**, Au ··· OSO_2CF_3 3.284(4) Å, is significantly longer than that of **9** as reported in the related series $[Au_2X_2(\mu\text{-dcpm})_2]$ and $[Au_2(\mu\text{-dcpm})_2]A_2$.[5a,b] Complex **10** displays two short C–H ··· O (anion) contacts of 2.39 Å (150.9°) and 2.48 Å (130.7°), that could be considered as hydrogen bonds.

Photoluminescence studies

The solid-state emission and excitation spectra for complexes **1**–**11** have been determined at 298 and 77 K and the results are summarised in Table 6. In Fig. 6 are plotted the solid state excitation and emission spectra of complex **4** (at 298 K). Only the organometallic monobridged digold(I) complex **4** $[(AuC_6F_5)_2(\mu\text{-}P^iPr_2CH_2PPh_2)]$ emits intensely at room temperature with emission maxima of 445 nm, whilst the other monobridged derivatives do not. At 77 K derivatives **1**–**4** are photoluminescent with the maxima in the range 440–486 nm, depending on the auxiliary ligand bonded to the diphosphine–gold fragment and following the series: C_6F_5 < Cl, Br < I, therefore totally different than predicted by the strength of the gold(I)–gold(I) interaction (emission maxima should be: C_6F_5 > Br > Cl). Additionally for complex **4** can be obtained two different emission spectra depending on the excitation frequency. The mononuclear gold(III) derivative **6** does not emit, which confirms the role of the gold(I) centres and of the gold(I)–gold(I) interactions. The dithiocarbamato–gold(I) complex **5** does not emit, which may be explained because secondary sulfur–gold bonds should red-shift the emission but this could disappear.[15,16]

Dinuclear doubly bridged complexes **7**–**11** are intensely luminescent at room and low temperature, as for the related

Table 6 Emission and excitation maxima (in nm) measured for complexes **1**–**11** in the solid state

	298 K		77 K	
Complex	λ_{exc}	λ_{em}	λ_{exc}	λ_{em}
1	–	–	320	456
2	–	–	325	457
3	–	–	342	471, 481
4	335	445	327	440
			350	440, 486
5	–	–	–	–
6	–	–	–	–
7	280–380	500	325	470, 520 (sh)
			380	508
8	320	480	322	469
	380	491, 527 (sh)		
9	393	513	346,387	499
10	334	482	325	459
11	340	478	335	463

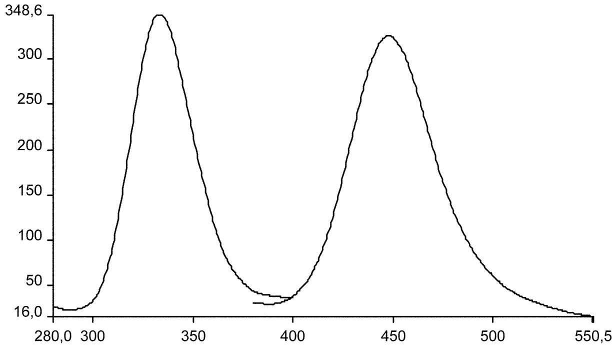

Fig. 6 Excitation and emission spectra in the solid state at 298 K of complex **4**; intensity in arbitrary units.

series $[Au_2(\mu\text{-P–P})_2]^{2+}$ (P–P = dppm, dcpm) with different anions. A second spectrum (less intense) is obtained by changing the excitation frequency for complexes **7** (at 77 K) and **8** (at 298 K). At room temperature the emission maxima range from 480 to 513 nm, in the sequence Br, ClO_4, CF_3SO_3 < Br (second spectrum) < Cl < I, whilst at low temperature the emission maxima are in the range 459–508 nm, in the sequence ClO_4, CF_3SO_3 < Br, Cl < I < Cl (second spectrum). In both cases the tendency is not the predicted by the strength of the gold–gold interaction. A blue-shift (from 11 to 30 nm) of the emission maxima is observed after lowering the temperature. When non-coordinating counter-ions are present, the results are the same but with coordinating halide anions, the emission depends on the nature of the anion, as was previously reported for related dinuclear derivatives.[3,5a,17] In these complexes we have not found the intense UV emission found in the similar doubly bridged dcpm digold derivatives (suggested to be the intrinsic gold–gold centred emission) and they emit only in the visible region, as reported for doubly bridged dppm digold derivatives. A deactivating state involving the phenyl rings has been invoked to explain this fact and could be also proposed for our unsymmetric diphosphine.[5b]

Experimental

General

All the reactions were carried out under an argon atmosphere at room temperature. IR spectra were recorded on a Perkin Elmer Spectrum One and a Brücker Equinox 55 spectrophotometers, over the range 4000–200 cm^{-1}, by using Nujol mulls between polyethylene sheets or KBr pellets. ^{1}H, ^{1}H{^{31}P}, ^{19}F and ^{31}P{^{1}H} NMR spectra were recorded on a Bruker ARX·300 or GEMINI 2000 apparatus in $CDCl_3$ solutions (if no other solvent is stated); chemical shifts are quoted relative to $SiMe_4$ (external, ^{1}H), $CFCl_3$ (external, ^{19}F) and 85% H_3PO_4 (external, ^{31}P). ^{31}P{^{1}H} NMR spectra of derivatives **7**–**11** were calculated by using the software package Swan-NMR 3.3.5. C, H, N and S analyses were performed with a Perkin-Elmer 2400 microanalyzer. Conductivities were measured in acetone solution with a Philips PW 9509 apparatus. Mass spectra were recorded on a VG Autospec using FAB technique (with Cs gun) and 3-nitrobenzyl alcohol as matrix. Emission and excitation spectra were measured in the solid state as finely pulverised KBr mixtures at room temperature and 77 K with a Perkin-Elmer LS-50B spectrofluorometer.

Preparation of $[(AuX)_2(\mu\text{-P}^i\text{Pr}_2\text{CH}_2\text{PPh}_2)]$ (X = Cl 1, Br 2, I 3, C_6F_5 4)

To a 10 mL dichloromethane solution of [AuX(tht)][18,19] (tht = tetrahydrothiophene; 0.2 mmol; X = Cl, 64 mg; C_6F_5 90 mg) or $[AuX(AsPh_3)]$[20] (0.2 mmol; X = Br, 117 mg; I 126 mg) was added diisopropylphosphine(diphenylphosphine)methane[21] (33 mg, 0.1 mmol). After stirring for 1 h, the solution was concentrated to *ca.* 3 mL. Addition of hexane (**1**, **2**, **4**) or diethyl ether (**3**) afforded complexes **1**–**4** as white solids, which were washed with more diethyl ether or hexane (2 × 5 mL). Yield of **1**: 75%. Λ: 3 ohm^{-1} cm^2 mol^{-1}. ^{1}H NMR: δ 1.18 (dd, 6H, $^3J_{HH}$ = 7.1, $^3J_{HP}$ = 19 Hz, CH_3), 1.26 (dd, 6H, $^3J_{HH}$ = 6.9, $^3J_{HP}$ = 17.2 Hz, CH_3), 2.37 (m, 2H, CH), 3.54 (dd, 2H, $^2J_{HP}$ = 10.5 and 11.9 Hz, CH_2), 7.6–8.1 (m, 10H, Ph); ^{31}P{^{1}H} NMR: δ 39.2 (d, $^2J_{PP}$ = 51.9 Hz, PPh_2), 54.4 (d, ^{i}PPr$_2$). IR: 326 (m, ν(Au–Cl)) cm^{-1}. Found: C, 28.8; H, 3.15. $C_{19}H_{26}Au_2Cl_2P_2$ requires: C, 29.2; H, 3.35%. LSIMS (*m*/*z*, %, assignment): 745 (76, $[M - Cl]^+$). Yield of **2**: 83%. Λ: 8 ohm^{-1} cm^2 mol^{-1}. ^{1}H NMR: δ 1.18 (dd, 6H, J_{HH} = 7.1, J_{HP} = 18.9 Hz, CH_3), 1.25 (dd, 6H, $^3J_{HH}$ = 6.9, $^3J_{HP}$ = 17.4 Hz, CH_3), 2.52 (m, 2H, CH), 3.53 (dd, 2H, $^2J_{HP}$ = 10.5 and 11.8 Hz, CH_2), 7.5–8.1 (m, 10H, Ph); ^{1}H{^{31}P} NMR: δ 1.19 (d, 6H, $^3J_{HH}$ = 7.1 Hz, CH_3), 1.25 (d, 6H, $^3J_{HH}$ = 6.9, CH_3), 2.52 (m, 2H, CH), 3.53 (s, 2H, CH_2). ^{31}P{^{1}H} NMR: δ 35.4 (d, $^2J_{PP}$ = 55.9 Hz, PPh_2), 51.4 (d, ^{i}PPr$_2$). Found: C, 26.5; H, 2.95. $C_{19}H_{26}Au_2Br_2P_2$ requires: C, 26.25; H, 3.0%. LSIMS (*m*/*z*, %, assignment): 791 (100, $[M - Br]^+$). Yield of **3**: 70%. Λ: 10 ohm^{-1} cm^2 mol^{-1}. ^{1}H NMR: δ 1.17 (dd, 6H, $^3J_{HH}$ = 7.3, $^3J_{HP}$ = 15.8 Hz, CH_3), 1.23 (dd, 6H, $^3J_{HH}$ = 7.3, $^3J_{HP}$ = 12.6 Hz, CH_3), 2.37 (m, 2H, CH), 2.81 ('t', 2H, $^2J_{HP}$ = 9.6 Hz, CH_2), 7.5–7.9 (m, 10H, Ph); ^{31}P{^{1}H} NMR: δ 32.6 (d, $^2J_{PP}$ = 62.9 Hz, PPh_2), 51.6 (d, ^{i}PPr$_2$). Found: C, 23.8; H, 2.8. $C_{19}H_{26}Au_2I_2P_2$ requires: C, 23.65; H, 2.7%. LSIMS (*m*/*z*, %, assignment): 837 (100, $[M - I]^+$). Yield of **4**: 75%. Λ: 7 ohm^{-1} cm^2 mol^{-1}. IR: 955, 792 (s, C_6F_5) cm^{-1}. ^{1}H NMR: δ 1.16 (dd, 6H, $^3J_{HH}$ = 7.1, $^3J_{HP}$ = 11.0 Hz, CH_3), 1.22 (dd, 6H, $^3J_{HH}$ = 7.1, $^3J_{HP}$ = 11.1 Hz, CH_3), 2.3 (m, 2H, CH), 2.84 ('t', 2H, $^2J_{HP}$ = 10.3 Hz, CH_2), 7.3–8.0 (m, 10H, Ph); ^{31}P{^{1}H} NMR: δ 39.5 (dm, $^2J_{PP}$ = 66.5 Hz, PPh_2), 54.8 (dm, ^{i}PPr$_2$); ^{19}F NMR: δ −117.5 (m, 2F$_o$), −117.7 (m, 2F$_o$), −160.2 (t, $^3J_{FF}$ = 20.0 Hz, 1F$_p$), −160.5 (t, $^3J_{FF}$ = 20.1 Hz, 1F$_p$), −164.2 (m, 4F$_m$). Found: C, 43.5; H, 2.65. $C_{37}H_{26}AuF_{15}P_2$ requires: C, 43.8; H, 2.6%. LSIMS (*m*/*z*, %, assignment): 877 (100, $[M - C_6F_5]^+$), 1044 (15, $[M]^+$).

Preparation of $[\{Au(S_2CN(CH_2Ph)_2)\}_2(\mu\text{-P}^i\text{Pr}_2\text{CH}_2\text{PPh}_2)]$ 5

To a dichloromethane solution (10 mL) of **1** (78 mg, 0.1 mmol) was added $NaS_2CN(CH_2Ph)_2$ (0.2 mmol, 59 mg). The mixture was stirred for about 2 h, then filtered through Celite. Concentration to *ca.* 2 mL and addition of cold 1 : 1 diethyl ether–hexane (20 mL) afforded complex **5** as a yellow solid. Yield: 67%. Λ: 15 ohm^{-1} cm^2 mol^{-1}. ^{1}H NMR: δ 1.18 (dd, 6H, $^3J_{HH}$ = 6.9, $^3J_{HP}$ = 17.4 Hz, CH_3), 1.26 (dd, 6H, $^3J_{HH}$ = 7.1, $^3J_{HP}$ = 17.4 Hz, CH_3), 2.3 (m, 2H, CH), 2.85 ('t', 2H, $^2J_{HP}$ = 10.7 Hz, CH_2), 5.12 (s, 8H, CH_2N), 7.3–8.1 (m, 30H, Ph); ^{31}P{^{1}H} NMR: δ 31.2 (d, $^2J_{PP}$ = 64.3 Hz, PPh_2), 54.4 (d, ^{i}PPr$_2$). Found: C, 47.25; H, 4.35; N, 2.05; S, 10.1. $C_{49}H_{54}Au_2N_2P_2S_4$ requires: C, 46.9; H, 4.35; N, 2.25; S, 10.2%. LSIMS (*m*/*z*, %, assignment): 982 (100, $[M - S_2CN(CH_2Ph)_2]^+$).

Table 7 Details of crystal data and structure refinement for complexes **1**, **2**, **4**, **9** and **10**

Compound	**1**·$CO(CH_3)_2$	**2**·$1.5CO(CH_3)_2$	**4**	**9**	**10**·$2CH_2Cl_2$
Empirical formula	$C_{22}H_{32}Au_2Cl_2OP_2$	$C_{23.5}H_{35}Au_2Br_2O_{1.5}P_2$	$C_{31}H_{26}Au_2F_{10}P_2$	$C_{38}H_{52}Au_2I_2P_4$	$C_{44}H_{60}Au_2Cl_4F_6O_6P_4S_2$
M_r	839.25	957.21	1044.39	1280.41	1522.65
T/K	133(2)	133(2)	100(2)	100(2)	100(2)
λ/Å	0.71073	0.71073	0.71073	0.71073	0.71073
Crystal system	Monoclinic	Monoclinic	Monoclinic	Monoclinic	Triclinic
Space group	$P2_1/c$	$C2/c$	$P2_1/c$	$P2_1/n$	$P\bar{1}$
Unit cell dimensions					
a/Å	14.9066(11)	19.7999(14)	12.9723(10)	12.1033(10)	10.0765(9)
b/Å	12.1750(8)	16.6728(12)	16.9452(13)	14.3905(12)	11.688(1)
c/Å	14.8415(11)	18.2896(12)	15.1980(11)	12.1366(9)	13.2223(12)
α/°	90	90	90	90	70.562(1)
β/°	97.518(3)	105.643(3)	108.926(2)	100.234(1)	69.619(2)
γ/°	90	90	90	90	89.378(2)
V/Å^3	2670.4(3)	5814.1(7)	3160.2(4)	2080.2(3)	1366.8(2)
Z	4	8	4	2	1
D_c/Mg m^{-3}	2.087	2.187	2.195	2.044	1.850
μ/mm^{-1}	11.306	12.956	9.456	8.708	5.814
F(000)	1576	3568	1960	1208	744
Crystal size/mm	0.17 × 0.13 × 0.07	0.20 × 0.16 × 0.07	0.28 × 0.20 × 0.18	0.38 × 0.26 × 0.20	0.18 × 0.10 × 0.10
Diffractometer	Bruker SMART 1000 CCD	Bruker SMART 1000 CCD	Bruker SMART APEX CCD	Bruker SMART APEX CCD	Bruker SMART APEX CCD
θ Range data collection/°	1.38–30.03.	1.62–30.03.	1.86–28.43.	2.19–28.42.	1.75–28.49.
Index ranges, hkl	−20 to 20, −17 to 17, −20 to 20	−27 to 27, −23 to 23, −25 to 25	−9 to 17, −22 to 22, −19 to 16	−13 to 15, −16 to 18, −16 to 9	−10 to 13, −15 to 13, −16 to 15
Reflections collected	47562	52984	20427	13318	9037
Independent reflections (R_{int})	7785 (0.0344)	8508 (0.0405)	7342 (0.0418)	4802 (0.1046)	6053 (0.0256)
Compl. to θ = 30.00° (%)	99.8	100.0	92.1	91.7	87.2
Absorption correction	SADABS	SADABS	SADABS	SADABS	SADABS
Max., min. transmission	0.564, 0.387	0.494, 0.283	1.0000, 0.6997	0.928, 0.408	1.000, 0.830
Data/restraints/parameters	7785/49/268	8508/67/284	7342/0/410	4802/0/212	6053/0/311
Goodness-of-fit on F^2	0.989	0.999	0.880	1.045	0.896
Final R indices [$I > 2\sigma(I)$]	$R1 = 0.0174$, $wR2 = 0.0374$	$R1 = 0.0199$, $wR2 = 0.0479$	$R1 = 0.0350$, $wR2 = 0.0534$	$R1 = 0.0583$, $wR2 = 0.1470$	$R1 = 0.0352$, $wR2 = 0.0692$
R indices (all data)	$R1 = 0.0239$, $wR2 = 0.0386$	$R1 = 0.0255$, $wR2 = 0.0491$	$R1 = 0.0494$, $wR2 = 0.0566$	$R1 = 0.0639$, $wR2 = 0.1501$	$R1 = 0.0434$, $wR2 = 0.0710$
Largest diff. peak, hole/e Å^{-3}	0.897, −0.616	1.427, −1.195	1.649, −1.178	3.270, −2.761	2.311, −1.374

Preparation of $\mathrm{[Au(C_6F_5)_3(P^iPr_2CH_2PPh_2)]}$ 6

To a dichloromethane solution (10 mL) of $\mathrm{[Au(C_6F_5)_3(tht)]}$[22] (79 mg, 0.1 mmol) was added diisopropylphosphine(diphenylphosphine)methane (33 mg, 0.1 mmol). After stirring for 1 h, the solution was concentrated to *ca.* 3 mL. Addition of cold hexane (10 mL) afforded **6** as a white solid. A second fraction was obtained by concentration and cooling to −18 °C. Yield: 70%. Λ: 5 ohm^{-1} cm^2 mol^{-1}. IR: 966, 792 (s, $\mathrm{C_6F_5}$) cm^{-1}. ^{1}H NMR: δ 1.10 (dd, 6H, $^3J_{HH} = 7$, $^3J_{HP} = 18.1$ Hz, CH$_3$), 1.16 (dd, 6H, $^3J_{HH} = 7$, $^3J_{HP} = 17.1$ Hz, CH$_3$), 2.40 (d, 2H, $^2J_{HP} = 10.8$ Hz, CH$_2$), 2.61 (m, 2H, CH), 7.3–7.6 (m, 10H, Ph); ^{1}H{^{31}P} NMR δ 1.10 (d, 6H, $^3J_{HH} = 7$ Hz, CH$_3$), 1.16 (d, 6H, CH$_3$), 2.40 (s, 2H, CH$_2$), 2.61 (sept, 2H, CH); ^{31}P{^{1}H} NMR: δ −27.5 (d, $^2J_{PP}$ = 24.3 Hz, PPh$_2$), 38.4 (m, ^{i}PPr$_2$); ^{19}F NMR: δ −120.2 (m, 4F$_o$), −123.1 (m, 2F$_o$), −156.9 (t, $^3J_{FF} = 20.0$ Hz, 2F$_p$), −158.4 (t, $^3J_{FF}$ = 20.1 Hz, 1F$_p$), −161 (m, 4F$_m$), −162.1 (m, 2F$_m$). Found: C, 35.7; H, 2.65. $\mathrm{C_{31}H_{26}Au_2F_{10}P_2}$ requires: C, 35.65; H, 2.5%. LSIMS (*m*/*z*, %, assignment): 847 (100, [M − C$_6$F$_5$]$^+$), 1015 (12, [M + H]$^+$).

Preparation of $\mathrm{[Au_2X_2(\mu\text{-}P^iPr_2CH_2PPh_2)_2]}$ (X = Cl 7, Br 8, I 9)

To a 10 mL dichloromethane solution of [AuCl(tht)] (64 mg, 0.2 mmol) or $\mathrm{[AuX(AsPh_3)]}$ (0.2 mmol; X = Br, 117 mg; I 126 mg) was added diisopropylphosphine(diphenylphosphine)methane (66 mg, 0.2 mmol). After stirring for 1 h, the solution was concentrated to *ca.* 3 mL. Addition of cold hexane (**7**) or diethyl ether (**8**–**9**) afforded the corresponding complexes as white (**7**–**8**) or yellow solids (**9**). A second fraction was obtained by concentration and cooling to −18 °C. Yield of **7**: 65%. Λ: 51 ohm^{-1} cm^2 mol^{-1}. ^{1}H NMR: δ 1.13 (m, 12H, CH$_3$), 1.27 (m, 12H, CH$_3$), 2.36 (br, 4H, CH), 3.9 (br, 4H, CH$_2$), 7.3–8.1 (m, 20H, Ph); ^{1}H{^{31}P} NMR: δ 1.13 (d, 12H, $^3J_{HH} = 6.9$ Hz, CH$_3$), 1.27 (d, 12H, CH$_3$), 2.36 (m, 4H, CH), 3.9 (s, 4H, CH$_2$); ^{31}P{^{1}H} NMR: head–head isomer: δ 33.2 (m, PPh$_2$), 59 (m, ^{i}PPr$_2$); head–tail isomer: δ 33.7 (dm, $^2J_{PP}$ = 245.3 Hz, PPh$_2$), 59.1 (dm, ^{i}PPr$_2$); ^{31}P{^{1}H} NMR (−50 °C): head–head isomer: δ 33.6 (‘t’, *N* = 23.7 Hz, PPh$_2$), 58.6 (‘t’, ^{i}PPr$_2$), with calculated ^2J(P^{i}Pr$_2$–P^{i}Pr$_2$), ^2J(PPh$_2$–PPh$_2$) = 260, 255 Hz, ^2J(PPh$_2$–P^{i}Pr$_2$) = 47.5 Hz; head–tail isomer: δ 33.9 (dd, $^2J_{PP}$ = 297.4 and 44 Hz, PPh$_2$), 58.6 (dd, ^{i}PPr$_2$). IR: 326 (m, ν(Au–Cl)) cm^{-1}. Found: C, 41.2; H, 4.55. $\mathrm{C_{38}H_{52}Au_2Cl_2P_4}$ requires: C, 41.6; H, 4.75. LSIMS (*m*/*z*, %, assignment): 745 (100, [M − Cl − P^{i}Pr$_2$CH$_2$PPh$_2$]$^+$), 1025 (77, [M − Cl$_2$ − H]$^+$). Yield of **8**: 77%. Λ: 71 ohm^{-1} cm^2 mol^{-1}. ^{1}H NMR: δ 1.11 (m, 12H, CH$_3$), 1.33 (m, 12H, CH$_3$), 2.46 (m, 4H, CH), 3.84 (br, 4H, CH$_2$), 7.3–8.1 (m, 20H, Ph); ^{1}H{^{31}P} NMR: δ 1.11 (d, 12H, $^3J_{HH} = 7$ Hz, CH$_3$), 1.33 (d, 12H, CH$_3$), 2.46 (m, 4H, CH), 3.84 (br, 4H, CH$_2$); ^{31}P{^{1}H} NMR: head–head isomer: δ 31.3 (‘t’, *N* = 27 Hz, PPh$_2$), 57.6 (‘t’, ^{i}PPr$_2$), with calculated ^2J(P^{i}Pr$_2$–P^{i}Pr$_2$), ^2J(PPh$_2$–PPh$_2$) = 278, 270 Hz, ^2J(PPh$_2$–P^{i}Pr$_2$) = 52 Hz; head–tail isomer: δ 31.7 (dd, $^2J_{PP}$ = 292.2 and 47 Hz, PPh$_2$), 57.7 (dd, ^{i}PPr$_2$). Found: C, 38.75; H, 4.45. $\mathrm{C_{38}H_{52}Au_2Br_2P_4}$ requires: C, 38.45; H, 4.4%. LSIMS (*m*/*z*, %, assignment): 789 (100, [M − Br − P^{i}Pr$_2$CH$_2$PPh$_2$]$^+$). Yield of **9**: 68%. Λ: 18 ohm^{-1} cm^2 mol^{-1}. ^{1}H NMR: δ 1.13 (m, 12H, CH$_3$), 1.31 (m, 12H, CH$_3$), 2.51 (m, 4H, CH), 3.81 (br, 4H, CH$_2$), 7.5–8.0 (m, 20H, Ph); ^{1}H{^{31}P} NMR: δ 1.13 (m, 12H, CH$_3$), 1.31 (m, 12H, CH$_3$), 2.51 (m, 4H, CH), 3.81 and 3.91 (s, 4H, CH$_2$); ^{31}P{^{1}H} NMR: head–head isomer: δ 27.7 (‘t’, *N* = 29 Hz, PPh$_2$), 53.1 (‘t’, ^{i}PPr$_2$), with calculated ^2J(P^{i}Pr$_2$–P^{i}Pr$_2$) = ^2J(PPh$_2$–PPh$_2$) = 264 Hz, ^2J(PPh$_2$–P^{i}Pr$_2$) = 56.5 Hz; head–tail isomer: δ 28.9 (dd, $^2J_{PP}$ = 282 and 54.1 Hz, PPh$_2$), 53.6 (dd, ^{i}PPr$_2$). Found: C, 35.85; H, 3.85. $\mathrm{C_{38}H_{52}Au_2I_2P_4}$ requires: C, 35.65; H, 4.1%. LSIMS (*m*/*z*, %, assignment): 837 (67, [M − I − P^{i}Pr$_2$CH$_2$PPh$_2$]$^+$).

Preparation of $\mathrm{[Au_2(\mu\text{-}P^iPr_2CH_2PPh_2)_2]A_2}$ A = $\mathrm{CF_3SO_3}$ 10, $\mathrm{ClO_4}$ 11

To a dichloromethane solution (10 mL) of $\mathrm{[Au(tht)_2]A}$[23] (0.2 mmol) prepared *in situ* was added diisopropylphosphine(diphenylphosphine)methane (66 mg, 0.2 mmol). After stirring for 1 h, the solution was concentrated to *ca.* 3 mL. Addition of cold diethyl ether–hexane (1 : 1) afforded derivatives **10**–**11** as white solids; a second fraction was obtained by concentration and cooling to −18 °C. Yield of **10**: 74%. Λ: 212 ohm^{-1} cm^2 mol^{-1}. ^{1}H NMR: δ 1.11 (m, 12H, CH$_3$), 1.34 (m, 12H, CH$_3$), 2.33 (m, 4H, CH), 3.80 (br, 4H, CH$_2$), 7.4–8.1 (m, 20H, Ph); ^{1}H NMR (in d$_6$-acetone): δ 1.35 (m, 24H, CH$_3$), 2.53 (m, 4H, CH), 4.18 (m, 4H, CH$_2$), 7.5–8.1 (m, 20H, Ph); ^{1}H{^{31}P} NMR: δ 1.11 (d, 12H, $^3J_{HH} = 7$ Hz, CH$_3$), 1.34 (d, 12H, CH$_3$), 2.33 (m, 4H, CH), 3.8 (br, 4H, CH$_2$); ^{1}H{^{31}P} NMR (in d$_6$-acetone): head–head isomer: δ 1.29 (d, 12H, $^3J_{HH} = 7$ Hz, CH$_3$), 1.37 (d, 12H, CH$_3$), 2.52 (sept, 4H, CH), 4.19 (s, 4H, CH$_2$); head–tail isomer: δ 1.33 (d, 12H, $^3J_{HH} = 7$ Hz, CH$_3$), 1.40 (d, 12H, CH$_3$), 2.62 (sept, 4H, CH), 4.18 (s, 4H, CH$_2$); ^{31}P{^{1}H} NMR: head–head isomer: δ 37.6 (‘t’, *N* = 23.1 Hz, PPh$_2$), 61.2 (‘t’, ^{i}PPr$_2$), with calculated ^2J(P^{i}Pr$_2$–P^{i}Pr$_2$), ^2J(PPh$_2$–PPh$_2$) = 295, 260 Hz, ^2J(PPh$_2$–P^{i}Pr$_2$) = 45 Hz; head–tail isomer: δ 37.6 (dd, $^2J_{PP}$ = 303.9 and 40 Hz, PPh$_2$), 62.2 (dd, ^{i}PPr$_2$). IR: 1253 (s) and 637 (s, CF$_3$SO$_3$) cm^{-1}. Found: C, 36.4; H, 4.0; S, 4.65. $\mathrm{C_{39}H_{52}Au_2F_3O_3P_4S}$ requires: C, 36.25; H, 3.95; S, 4.85%. Yield of **11**: 70%. Λ: 145 ohm^{-1} cm^2 mol^{-1}. ^{1}H NMR: δ 1.09 (m, 12H, CH$_3$), 1.37 (m, 12H, CH$_3$), 2.29 (m, 4H, CH), 3.64 (br, 4H, CH$_2$), 7.5–8.0 (m, 20H, Ph); ^{1}H{^{31}P} NMR: head–head isomer: δ 1.09 (d, 12H, $^3J_{HH} = 7$ Hz, CH$_3$), 1.36 (d, 12H, CH$_3$), 2.33 (sept, 4H, CH), 3.64 (s, 4H, CH$_2$); head–tail isomer: δ 1.09 (d, 12H, $^3J_{HH}$ = 7 Hz, CH$_3$), 1.36 (d, 12H, CH$_3$), 2.27 (sept, 4H, CH), 3.63 (s, 4H, CH$_2$); ^{31}P{^{1}H} NMR: head–head isomer: δ 36.5 (‘t’, *N* = 23.2 Hz, PPh$_2$), 59.6 (‘t’, ^{i}PPr$_2$), with calculated ^2J(P^{i}Pr$_2$–P^{i}Pr$_2$), ^2J(PPh$_2$–PPh$_2$) = 294, 261 Hz, ^2J(PPh$_2$–P^{i}Pr$_2$) = 48 Hz; head–tail isomer: δ 36.7 (dd, $^2J_{PP}$ = 306.2 and 45.9 Hz, PPh$_2$), 60.8 (dd, ^{i}PPr$_2$); ^{19}F NMR: δ −78.9 (s, CF$_3$). IR: 1092 (s) and 623 (s, ClO$_4$) cm^{-1}. Found: C, 36.9; H, 4.5. $\mathrm{C_{38}H_{52}Au_2Cl_2O_8P_4}$ requires: C, 37.25; H, 4.25%.

Crystal structure determination of 1, 2, 4, 9 and 10

Some crystallographic data of $\mathrm{[(AuX)_2(\mu\text{-}P^iPr_2CH_2PPh_2)]}$ (X = Cl, Br, C$_6$F$_5$), $\mathrm{[Au_2I_2(\mu\text{-}P^iPr_2CH_2PPh_2)_2]}$ and $\mathrm{[Au_2(\mu\text{-}P^iPr_2CH_2PPh_2)_2](CF_3SO_3)_2}$ are given in Table 7. The structures were refined anisotropically (full-matrix least-squares) on F^2 (program SHELXL-97)[24] using a system of restraints (to light-atom *U* values and local ring symmetry) for complexes **1** and **2**. All non-hydrogen atoms were refined anisotropically. Hydrogen atoms were included using a riding model. *Special details of refinement for* **2**: The second acetone molecule is disordered over a twofold axis; it was refined isotropically without hydrogens.

CCDC reference numbers 216496–216500.

See http://www.rsc.org/suppdata/dt/b3/b309116c/ for crystallographic data in CIF or other electronic format.

Acknowledgements

We thank the Dirección General de Investigación Científica y Técnica (project BQU2001–2409-C02–01) and the Fonds der Chemischen Industrie for financial support. We also thank Dr J. Galbán (Universidad de Zaragoza, Spain) for kindly providing apparatus facilities.

References

1 (*a*) P. Pyykkö, *Chem. Rev.*, 1997, **97**, 597; (*b*) H. Schmidbaur, *Gold Bull.*, 2000, **33**, 3.

2 (*a*) P. Pyykkö, N. Runeberg and F. Mendizabal, *Chem. Eur. J.*, 1997, **3**, 1451, and references therein; (*b*) P. M. Van Calcar, M. M. Olmstead and A. L. Balch, *J. Chem. Soc., Chem. Commun.*, 1995, 1773; (*c*) Z. Assefa, B. G. McBurnett, R. J. Staples, J. P. Fackler, Jr., B. Assmann, K. Angermaier and H. Schmidbaur, *Inorg. Chem.*, 1995, **34**, 75; (*d*) H. Ecken, M. M. Olmstead, B. C. Noll, S. Attar, B. Schlyer and A. L. Balch, *J. Chem. Soc., Dalton Trans.*, 1998, 3715; (*e*) D. V. Toronto, B. Weissbart, D. S. Tinti and A. L. Balch,

Inorg. Chem., 1996, **35**, 2484; (*f*) M. Bardají, P. G. Jones and A. Laguna, *J. Chem. Soc., Dalton Trans.*, 2002, 3624.

3 C. King, J. C. Wang, M. N. I. Khan and J. P. Fackler, Jr., *Inorg. Chem.*, 1989, **28**, 2145.

4 (*a*) J. M. Forward, J. P. Fackler, Jr. and Z. Assefa, *Optoelectronic Properties of Inorganic Compounds*, ed. D. M. Roundhill, J. P. Fackler, Jr., Plenum Press, London, 1998, p. 195; (*b*) V. W.-W. Yam and K. K.-W. Lo, *Chem. Soc. Rev.*, 1999, **28**, 323.

5 (*a*) W.-F. Fu, K.-C. Chan, V. M. Miskowski and C.-M. Che, *Angew. Chem., Int. Ed.*, 1999, **38**, 2783; (*b*) W.-F. Fu, K.-C. Chan, K.-K. Cheung and C.-M. Che, *Chem. Eur. J.*, 2001, **7**, 4656; (*c*) H.-X. Zhang and C.-M. Che, *Chem. Eur. J.*, 2001, **7**, 4887.

6 R. Usón, A. Laguna, M. Laguna, M. N. Fraile, P. G. Jones and G. M. Sheldrick, *J. Chem. Soc., Dalton Trans.*, 1986, 291.

7 R. Usón, A. Laguna, J. García and M. Laguna, *Inorg. Chim. Acta*, 1979, **37**, 201.

8 (*a*) X. Hong, K. K. Cheung, C.-X. Guo and C. M. Che, *J. Chem. Soc., Dalton Trans.*, 1994, 1867; (*b*) N. C. Payne, R. Ramachandran and R. J. Puddephatt, *Can. J. Chem.*, 1995, **73**, 6; (*c*) P. G. Jones and C. Thöne, *Chem Ber.*, 1991, **124**, 2725; (*d*) H. Piana, H. Wagner and U. Schubert, *Chem. Ber.*, 1991, **124**, 63; (*e*) P. G. Jones and C. Thöne, *Acta Crystallogr., Sect. C*, 1992, **48**, 1312.

9 M. C. Gimeno and A. Laguna, *Chem. Rev.*, 1997, **97**, 511.

10 (*a*) E. W. Garbisch, Jr., *J. Chem. Educ.*, 1968, **45**, 480; (*b*) H. Günther, *NMR Spectroscopy. Basic Principles, Concepts, and Applications in Chemistry*, John Wiley & Sons, Chichester, 2nd edn., 1995, p. 181; (*c*) M. Bardají, A. Laguna and M. Laguna, *J. Chem. Soc., Dalton Trans.*, 1995, 1255.

11 J. Shain and J. P. Fackler, *Inorg. Chim. Acta*, 1987, **131**, 157.

12 M. N. I. Khan, C. King, D. D. Heinrich, J. P. Fackler, Jr. and L. C. Porter, *Inorg. Chem.*, 1989, **28**, 2150.

13 H. R. C. Jaw, M. M. Savas, R. D. Rogers and W. R. Mason, *Inorg. Chem.*, 1989, **28**, 1028.

14 H. Schmidbaur, A. Wohlleben, U. Schubert, A. Frank and G. Huttner, *Chem. Ber.*, 1977, **110**, 2751.

15 M. Bardají, A. K. Fischer, P. G. Jones and A. Laguna, *Inorg. Chem.*, 2000, **39**, 3560.

16 M. Bardají, J. Vicente, A. Laguna and P. G. Jones, *Inorg. Chem.*, 2001, **40**, 2675.

17 H. Xiao, Y.-X. Weng, W.-T. Wong, T. C. W. Mak and C.-M. Che, *J. Chem. Soc., Dalton Trans.*, 1997, 221.

18 R. Usón, A. Laguna and M. Laguna, *Inorg. Synth.*, 1989, **26**, 85.

19 R. Usón, A. Laguna and J. Vicente, *Chem. Commun.*, 1976, 353.

20 C. A. McAuliff, R. V. Parish and P. D. Randal, *J. Chem. Soc., Dalton Trans.*, 1979, 1730.

21 S. O. Grim and J. D. Mitchell, *Inorg. Chem.*, 1977, **16**, 1770.

22 R. Usón, A. Laguna and M. Laguna, *Inorg. Synth.*, 1989, **26**, 87.

23 M. Bardají, P. G. Jones and A. Laguna, *Eur. J. Inorg. Chem.*, 1998, 989.

24 G. M. Sheldrick, SHELXL 97: A Program for Crystal Structure Refinement, University of Göttingen, Göttingen, Germany, 1997.